Model validation and integrated modelling simulations for the JT-60SA tokamak

G. Giruzzi[1], J. Garcia[1], N. Hayashi[2], M. Schneider[1], J.F. Artaud[1], M. Baruzzo[3], T. Bolzonella[3], D. Farina[4], L. Figini[4], T. Fujita[2], A. Fukuyama[5], S. Ide[2], E. Joffrin[1], X. Litaudon[1], S. Nowak[4], Y. Sakamoto[2], C. Sozzi[4], T. Suzuki[2], H. Urano[2], JT-60SA Research Plan contributors, the JT-60SA Team, the JT-60 Team and JET EFDA contributors*[6]

[1] *CEA, IRFM, 13108 Saint-Paul-lez-Durance, France*
[2] *Japan Atomic Energy Agency, Mukouyama, Naka City, Ibaraki, 311-0193 Japan*
[3] *Associazione EURATOM-ENEA, Consorzio RFX, 35127 Padova, Italy*
[4] *Istituto di Fisica del Plasma CNR, Euratom Association, 20125 Milano, Italy*
[5] *Graduate School of Engineering, Kyoto University, Kyoto, Japan*
[6] *JET-EFDA, Culham Science Centre, Abingdon, OX14 3DB, UK*

**See the Appendix of F. Romanelli et al., Proc. of the 24th IAEA Fusion Energy Conference 2012, San Diego, US*

e-mail contact of main author: gerardo.giruzzi@cea.fr

Abstract. A coordinated Japan-EU modelling activity has started in order to provide predictive simulations of the main JT-60SA scenarios. The first results of this activity are discussed in this paper. This includes: i) the critical comparison and benchmark of Japanese and EU H&CD codes, in particular of NBI codes for the complex injector configuration of the JT-60SA machine; ii) the validation of the main models and simulation framework used in both Japanese and EU integrated modelling suites of codes, based on selected reference discharges of JT-60U and JET, representing the main scenarios (H-mode, hybrid, advanced); iii) predictive modelling of JT-60SA scenario, using the 0.5-D code METIS.

1. Introduction

JT-60SA is a large fully superconducting new tokamak device being built under the Broader Approach Satellite Tokamak Programme jointly by Europe and Japan, and under the Japanese national programme [1]. The JT-60SA tokamak will be at the forefront of the international fusion programme for many years, both before and during the D-T phase of the ITER operation. It will support the ITER experimental programme as a satellite machine and at the same time provide key information for the design of DEMO scenarios. The preparation of its scientific programme is now progressing in the framework of a Japan-EU collaboration and will progressively integrate advances coming both from experiments and from theoretical developments [2,3]. As for ITER and DEMO, integrated modelling of full discharges will be the main ingredient to perform this preparation effectively and on a coherent basis. It is also a key element for minimizing the risks of such large and costly projects. In this framework, a coordinated Japan-EU modelling activity has started with the main goal of providing predictive simulations of the reference JT-60SA scenarios that could help in a detailed definition of the properties of various machine subsystems (H&CD, control coils, diagnostics) and at the same time could represent a reliable starting point for plasma operation. In EU, this activity takes place in the framework of the EFDA Integrated Scenario Modelling group.

The first milestone of this activity is the critical comparison and benchmark of Japanese and EU models and codes used for integrated tokamak modelling. This is a natural extension of activities already carried out in the framework of ITPA [4,5]. The benchmark of the H&CD codes, in particular of NBI codes, for the complex injector configuration of the JT-60SA machine is discussed in Sec. 2. ECCD operation diagrams obtained by extensive calculations with beam-tracing codes are also presented in Sec. 2.

The second milestone is the validation of the main models and simulation framework used in both Japanese and EU integrated modelling suites of codes. These include, e.g., energy and particle transport models, pedestal models, rotation sources and transport, synthetic diagnostics. JT-60SA is a machine designed on the basis of the results of JT-60U, and using an upgrade of the JT-60U NBI system. On the other hand, it has practically the same size as JET, which also has NBI as the main H&CD system. Therefore, it appears that simulations of JT-60SA scenarios should be based at least on experimental results of the two machines that are the most similar, for size and configuration: JT-60U and JET. On this basis, a validation exercise has been undertaken, involving the following steps:
- an agreement has been established for data exchange of reference JT-60U and JET shots, representing the main scenarios (H-mode, hybrid, advanced).
- various options for transport, pedestal, rotation models and scalings have been selected
- predictive simulations of the reference shots are being performed with both Japanese and EU codes and models with the aim of finding a unified modelling framework that works for both machines: this should give the maximum confidence for prediction of JT-60SA scenarios.

The first results of this comparison will be presented and discussed in Sec. 3, with particular emphasis on the transport model comparison.

The third milestone is the predictive modelling of JT-60SA scenarios, logically to be carried out after the previous steps are completed. Nevertheless, preparation of this activity has been done by simpler models, both 0-D and 0.5-D. In fact, integrated modelling of tokamak discharges is based on a hierarchy of simulation codes, each level of accuracy being used in

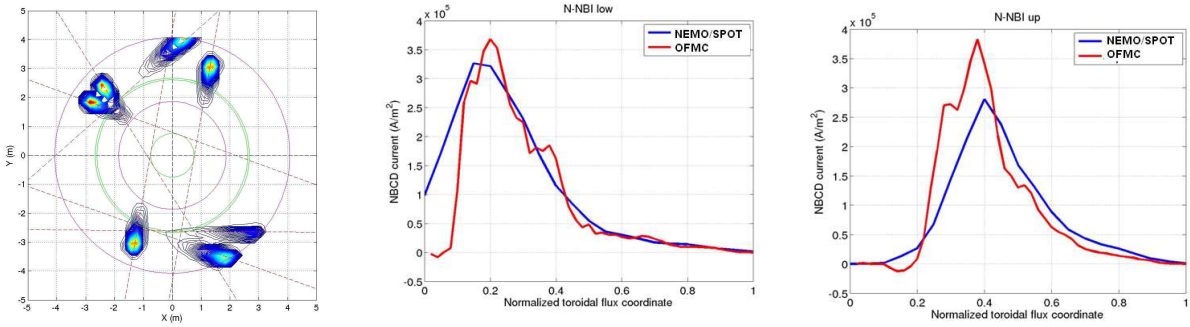

Fig. 1 : *Left : toroidal view of the power deposition profiles of the JT-60SA injected Neutral Beams, computed by means of the NEMO/SPOT code. Middle : driven current profiles computed by NEMO/SPOT and by F3D-OFMC for the lower Negative neutral beam ; right : the same for the upper beam.*

order to prepare and rationalize the higher simulation level. For instance, at CEA/Cadarache, this hierarchy consists of the codes HELIOS (0-D) [6], METIS (0.5-D) [7] and CRONOS (1.5-D) [8]. In particular, sets of simulations of the main JT-60SA scenarios [2,3] have been performed with the 0.5-D code METIS, which computes the time evolution of the global plasma quantities, equilibria and profiles, with simplified treatment of the sources and of spatial dependences. Results of these simulations are discussed in Sec. 4.

2. Computation of heating power depositions and driven currents

The JT-60SA H&CD system is described in [3] (Appendix A). The NBI system consists of twelve positive-ion-based (P-NBI) and two negative-ion-based NBI (N-NBI) units. The P-NBI system includes eight perpendicular, two co-tangential, and two counter-tangential injection units with beam energy of 85 keV and beam power of 2 MW/unit. The N-NBI system consists of two units (upper and lower) with beam energy of 500 keV and beam power of 5 MW/unit. A toroidal view of the power absorption of the various beams is shown in Fig. 1 (left). Power deposition and driven currents for a reference H-mode plasma (Scenario 2) have

been computed by means of the Japanese code F3D-OFMC [9] and of the EU code NEMO/SPOT [5,10]. The two codes give very similar results for the same plasma profiles, the little differences observed have been identified as mainly due to differences in the equilibria. As an example, the N-NBI driven current density profiles for the two N-NBI injectors, computed by the two codes, are shown in Fig. 1 (middle and right panels).

The nominal ECRH power available on JT-60SA will be 7 MW, delivered by dual frequency gyrotrons (110 and 138 GHz). The ECRH system will have various important functions in the JT-60SA scenarios, in particular for discharge startup and plasma control. Extensive computations have been performed with the EU beam-tracing code GRAY [11], both for benchmarking with the corresponding Japanese ray-tracing code [12] and in order to develop operation diagrams for the various scenarios. An example of such diagrams for the steady-state high-beta Scenario 5-1 is shown in Fig. 2 (left) : the diagram presents both the normalised radius location of maximum power absorption (black contours) and the driven current per unit power (colour contours) in the plane of poloidal (α) and toroidal (β) injection angles. One of the main applications of ECCD will be the control of NTMs. The power required for full island suppression by ECCD in Scenario 5, computed by the GREF code [13] is shown as a function of the EC beam width in Fig. 2 (right). These computations show that the EC power available in the initial phase of the JT-60SA exploitation (3 MW) should be sufficient for NTM suppression.

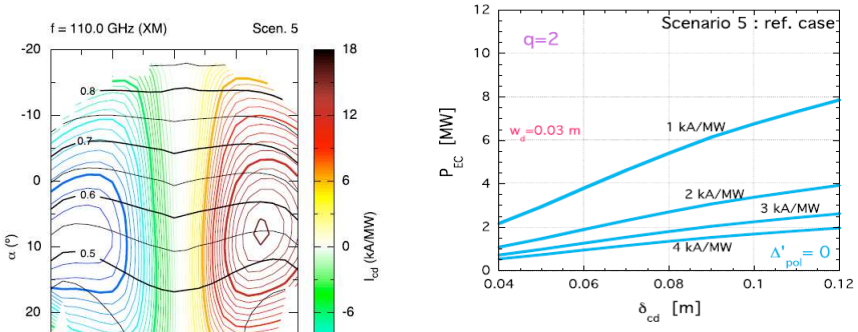

Fig. 2 : *Left : Black contours represent radius ρ where the EC deposition occurs. The colour contour plots represent the driven current in kA/MW. Right :EC power needed to stabilize the 2/1 mode versus the full beam width* δ_{cd}

3. Model validation using JT-60U and JET discharges

In order to validate the simulation framework to be used for JT-60SA scenario modelling, representative discharges of the three main operational scenarios, H-mode, hybrid and steady-state, have been selected for JT-60U and JET. A subset of these discharges is discussed here: their main parameters can be found in Table 1. Predictive simulations have been carried out with two transport models, CDBM [14] and GLF23 [15], and by adjusting, as a first step, the pedestal, rotation and density to experimental values whenever available. To carry out this programme, the integrated modelling codes CRONOS [8] and TOPICS-IB [16] are used.

In the CDBM transport model, a modification has been implemented in order to take into account the relatively high fast ion population in some of the discharges. For this purpose, the fast ion pressure is included in the normalized pressure gradient α of the shear function F(s,α) [14] and the gradient α_{th} only including the thermal plasma is used in the other terms. The original heat diffusivities [14] are modified as follows (quantities are defined in [14]):

$$\chi_{CDBM} = 12\frac{c^2}{\omega_{pe}^2}\frac{v_A}{qR}\alpha_{th}^{3/2}F(s,\alpha)G(\kappa)\text{, where } G(\kappa)=(2\kappa^{1/2}/(\kappa^2+1))^{3/2}$$

Two discharges from JT-60U, H-mode #33655 and Hybrid #48158, have been analyzed with CRONOS and TOPICS, using GLF23 and CDBM. The density and q profiles for both discharges are shown in Fig. 3 (left panels). The q profile is kept fixed during the simulation and just the temperatures are predicted. With CRONOS and for the GLF23 model, also the density is predicted and is shown in Fig. 3. The NBI power is calculated by means of the F3D-

OFMC code [9]. In Fig. 4, the results are compared to the experimental data, showing a good agreement between the two codes and for both the electron and ion temperatures for the H-mode discharge 33655. On the other hand, for the Hybrid shot 48158, both codes give similar results, leading to lower temperatures than expected for the case of CDBM and GLF23 without ExB effect, for which even a broad region with flat temperatures appear. However, when the ExB shear effect is included, the electron temperature is well simulated whereas the ion temperature is strongly overestimated. This indicates that the ExB shear effect plays an important role for this shot, but it is probably overestimated by GLF23, as it also happens for JET shots [17]. For ions, a better overall agreement is obtained by CDBM (Fig. 4d).

Discharge	q_{95}	κ/δ	Bt (T)	β_N	n/n_{Gw}	Ip (MA)	Pin (MW)
H-mode JT-60U #33655	3.0	1.53/0.16	3.1	1.1	0.48	1.8	10
Hybrid JT-60U #48158	3.0	1.40/0.33	1.5	2.6	0.54	0.9	9.5
H-mode JET #73344	3.5	1.75/0.40	2.7	1.5	0.75	2.5	12
Hybrid JET #77280	5.0	1.75/0.38	2.7	2.4	0.55	1.1	11

***Table 1**: Main characteristics of JT-60U shots 33655, 48158 and JET 73344, 77280, where κ/δ is the elongation/triangularity, Bt is the magnetic field in the axis, β_N is the normalized beta, n/n_{Gw} is the Greenwald fraction, Ip is the plasma current and Pin the injected power*

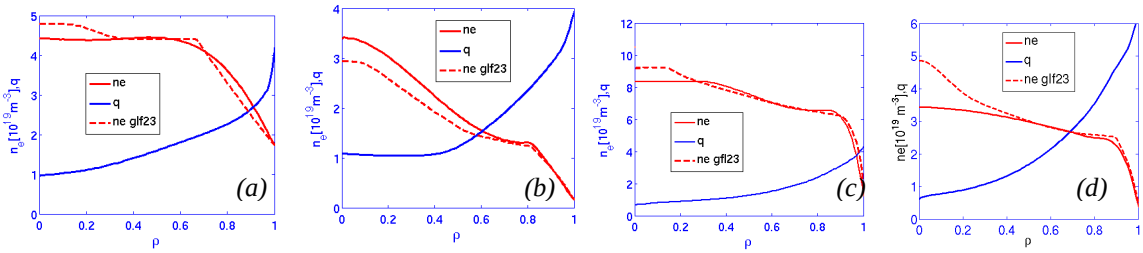

***Fig. 3**: Density and q profiles used for JT-60U shots 33655 (a) 48158 (b) and JET shots 73344 (c) and 77280 (d). Dashed lines are densities simulated by CRONOS with the GLF23 model.*

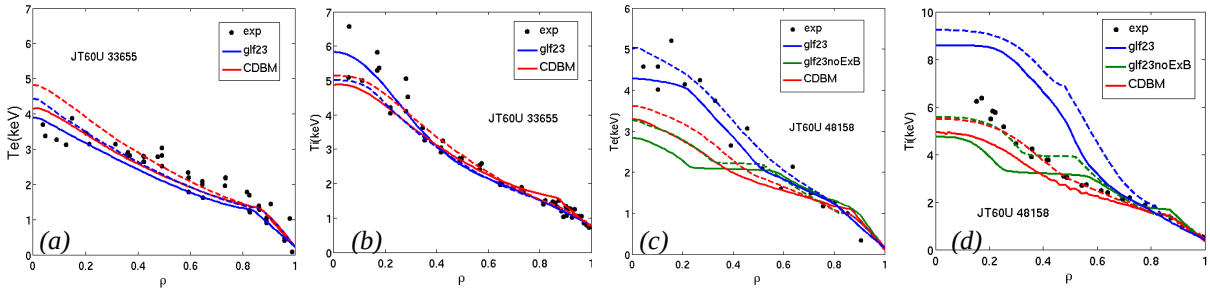

***Fig. 4**: Comparison between the electron (a,c) and ion (b,d) temperatures profiles with those obtained with CRONOS (solid) and TOPICS (dashed) with GLF23 and CDBM transport models for shot 33655 and 48158.*

Two discharges from JET, H-mode #73344 and Hybrid #77280, have been analyzed with CRONOS by using the same transport models. The density and q profiles for both discharges at t=19s for 73344 and 7.8s for 77280 are shown in Fig. 3 (right panels). The general procedure of the simulations is the same as for JT-60U, however in this case the experimental rotation profile has been used to evaluate the ExB shear, since it is available, and the NBI power is calculated by means of the NEMO/SPOT code [5,10]. In Fig. 5, the results are compared to the experimental data. There is a general good agreement for both electrons and ions, with some slightly lower temperatures for the CDBM transport model. GLF23 is the model that gets closest to the experimental data, although it overestimates the ion temperature to some extent. This feature has been found in many other hybrid JET discharges [17] and it is due to a too strong effect of rotation on confinement obtained with that transport model. For the

shot 77280, with higher fast ion contribution than the H-mode 73344, the CDBM transport model shows better agreement when the correction due to the fast ion population is applied.

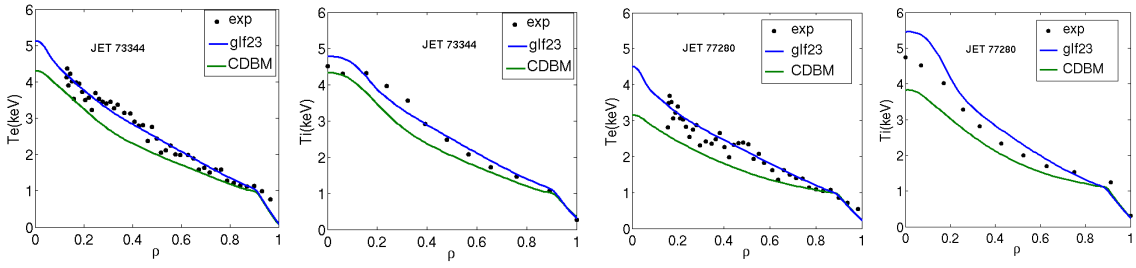

Fig. 5*: Comparison between the electron and ion temperatures profiles obtained by CRONOS with GLF23 and modified CDBM transport models for shots 73344 and 77280.*

In summary, although this work is still in progress, some trends start to appear. In general, the H-modes are well simulated for both devices with both GLF23 and CDBM. On the other hand, hybrid regimes seem to be more difficult to reproduce. In this case, GLF23 leads to the most reliable results for JET, although it starts to deviate from experimental data mainly for ions. In the case of JT-60U such deviations become larger. It is worth to point out that the amendment of the CDBM transport model that has been done in order to account for the superthermal pressure seems to be important, since otherwise the predicted temperatures would deviate even more substantially from the experimental data, due to the higher heat diffusivities.

The work shown here is just the initial step towards a full analysis of the physics differences between JT-60U and JET plasmas. This work will involve the simulation of additional discharges in order to analyse different plasma conditions, the simulation of the shots with the Bohm-GyroBohm model, the simulation of density, rotation and pedestal. The ExB shear effect can be introduced into the CDBM model [18] and the model will be applied especially to hybrid discharges. If successful, this exercise will provide a sound basis for scenario prediction in future devices as JT-60SA and ITER.

4. Simulations of the JT-60SA scenarios with the METIS code

METIS [7] computes the time evolution of the global plasma quantities for given waveforms of the control parameters. It solves the current diffusion equation taking into account an approximate equilibrium evolution. This approach allows completing the 0-D analysis with radial profiles and time evolutions, although with less accurate results than with a full 1.5-D code (which typically takes 10^3 - 10^4 times larger computation times). METIS simulations for JT-60SA have the following main characteristics:

1. a 2-D, time-dependent equilibrium is used, but based on equations for the time evolution of equilibrium moments: radii, elongation, triangularity, Shafranov shift, etc., using the separatrix computed by the TOSCA free-boundary equilibrium code [19]
2. heat transport coefficients are renormalized in order to enforce prescribed confinement scaling laws (in particular, L and H-mode in the various phases of the discharge)
3. the full current diffusion equation is solved numerically
4. density and temperature profiles are obtained by simplified solutions of the transport equations: discrete time slices are considered, on which stationary equations are solved. Pedestal values are imposed, consistent with pedestal scaling laws [20].
5. a coarse time-space grid (typically 300 x 21) is used in order to minimize the computation time (~ 1 minute per simulation).

The main parameters of the JT-60SA reference scenarios are shown in Table 2. They include both H-mode (#1, 2, 3, 4-1) and advanced scenarios (#4-2, 5-1, 5-2, 6). All of them

have been simulated by the METIS code, and the global parameters compared with those presented in Ref. [3], that have been obtained by means of the ACCOME code [21] with assigned density and temperature profiles. The main global quantities computed by METIS are shown in Table 3. They compare very well with those presented in [3].

	#1 Inductive	#2 Inductive	#3 High density	#4-1 ITER-like	#4-2 Advanced Inductive	#5-1 High β Full-CD	#5-2 High β,f_G Full-CD	#6 300s High β
configuration	DN	SN	SN	SN	SN	SN	SN	SN
I_p (MA)	5.5	5.5	5.5	4.6	3.5	2.3	2.1	2.0
B_T (T)	2.25	2.25	2.25	2.28	2.28	1.72	1.62	1.41
R/a (m)	2.96/ 1.18	2.96/ 1.18	2.96/ 1.18	2.93/ 1.14	2.93/ 1.14	2.97/ 1.11	2.96/ 1.12	2.97/1.11
k / δ	1.95/ 0.53	1.87/ 0.50	1.86/ 0.50	1.81/ 0.41	1.80/ 0.41	1.90/ 0.47	1.91/ 0.45	1.91/0.51
V (m^3)	132	131	131	122	122	124	124	124
q_{95}	3	3	3	3	4.4	5.8	6	4
$H_{98(y,2)}$	1.3	1.3	1.1	1.1	1.2	1.3	1.38	1.3
P_{add} (MW) $P_{NNB}/P_{PNB}/P_{EC}$	41 10/24/7	41 10/24/7	30 10/20/0	34 10/24/0	37 10/20/7	37 10/20/7	30 6/17/7	13.2 3.2/6/4
$\bar{n}_e$ ($10^{19}m^{-3}$) /f_G	6.3 / 0.5	6.3 / 0.5	10 / 0.8	9.1 / 0.8	6.9 / 0.8	5.0 / 0.85	5.3 / 1.0	2.0 / 0.39

Table 2: *Main parameters of the JT-60SA reference scenarios. DN, SN: double null, single null confirgurations*

	#1 Inductive	#2 Inductive	#3 High density	#4-1 ITER-like	#4-2 Advanced Inductive	#5-1 High β Full-CD	#5-2 High β,f_G Full-CD	#6 300s High β
β_N	3.5	3.5	2.6	2.8	3.1	4.4	4.2	3.3
β_p	0.87	0.76	0.68	0.86	1.36	1.88	2.60	0.91
$\langle T_e \rangle / \langle T_i \rangle$ (keV)	5.7/ 6.2	5.7/ 6.2	3.4/ 3.6	3.3/ 3.5	3.5/ 3.4	2.9/ 2.8	2.5/ 2.4	3.1/2.7
f_{bs}	0.25	0.24	0.22	0.27	0.41	0.61	0.74	0.32
f_{ni}	0.48	0.47	0.30	0.38	0.65	1.01	1.05	0.67

Table 3: *Main global quantities computed by the METIS code for the reference JT-60SA scenarios: normalised beta, poloidal beta, volume-averaged temperatures, bootstrap and non-inductive fractions.*

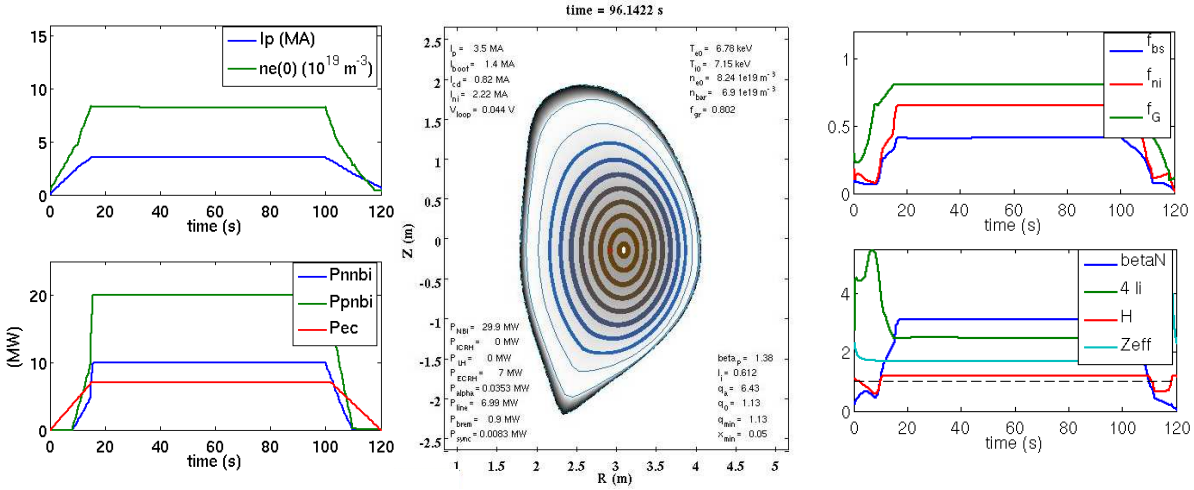

Fig. 6: *METIS simulations of Scenario 4-2 (advanced inductive). Time evolution of plasma current and central electron density (top left); time evolution of heating powers - positive NBI, negative NBI and ECRH (bottom left); magnetic equilibrium at the end of the flat-top phase (middle). Time evolution of bootstrap, non-inductive and Greenwald fractions (top right); time evolution of β_N, $4l_i$, H factor and Z_{eff} (bottom right).*

Examples of profiles and equilibria obtained by METIS are shown in Figs. 6, 7 for the advanced inductive (or hybrid) scenario 4-2 and in Figs. 8, 9 for the high-beta, fully non-inductive scenario 5-1. The heating power is a combination of positive NBI, negative NBI and EC waves, assumed to be deposited at normalised radius ρ ~ 0.4-0.5, in agreement with full

NBI computations. The ECCD profiles and efficiencies, estimated on the basis of simple analytical formulas, have been checked by means of ray-tracing calculations, for wave frequencies of 138 or 110 GHz depending on the magnetic field values.

Note that for both scenarios the flat-top duration ~ 100 s is sufficient to obtain stationary l_i and q-profiles. The negative NBI system is designed in order to drive non-inductive off-axis current, which effectively provides the scenarios with the desired q-profiles, i.e., flat and sawtooth-free for the advanced inductive scenario and reversed for the fully non-inductive. The detailed shape of the q-profile generally can be optimised by adjusting the timing of the application of NBI during the current ramp-up phase, as well as the location of the ECCD current. To this end, METIS allows efficient exploration of the impact of these parameters on the final q-profile, owing both to its computational speed and to the accurate solution of the current diffusion equation. These simulations performed with the METIS code constitute a preliminary exploration of the JT-60SA scenarios properties and at the same time the basis for a future extensive scenario simulation activity. They have already been used to initiate full ASTRA and JETTO 1.5D simulations for JT-60SA [22].

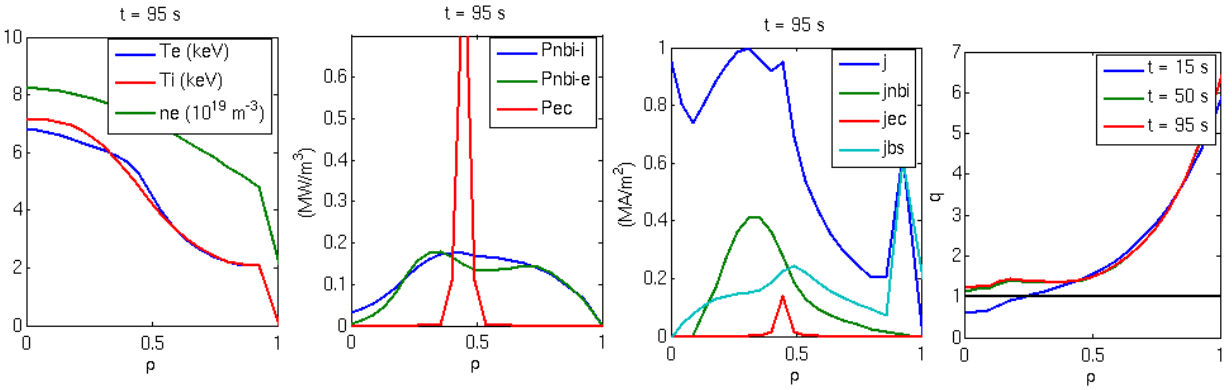

Fig. 7: *METIS simulations of Scenario 4-2 (advanced inductive). From left to right: temperature and density profiles at t = 95s; power deposition profiles (NBI power to ions and to electrons, EC power); current density profiles; safety factor profile evolution.*

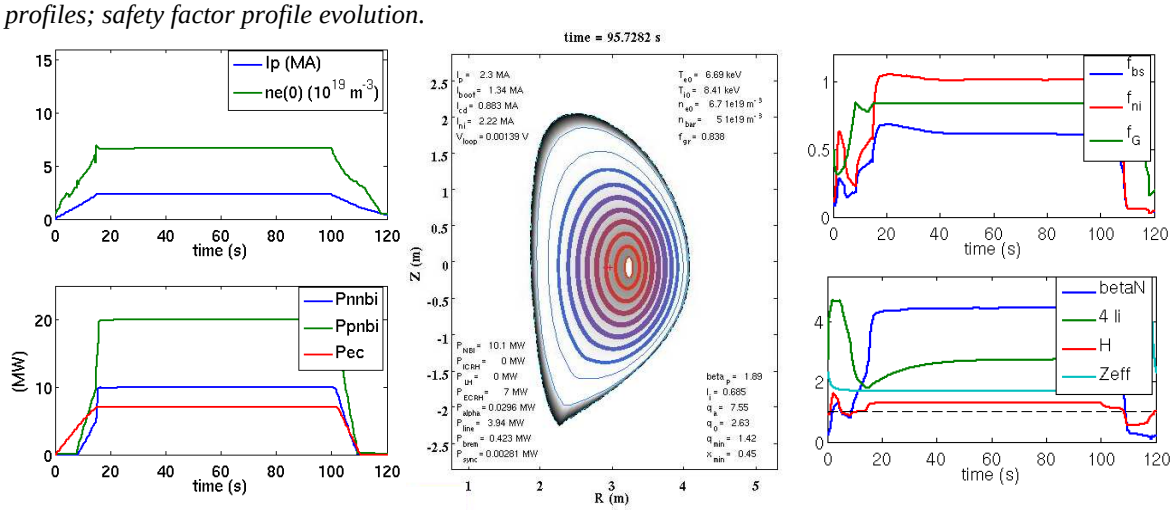

Fig. 8: *As in Fig. 6, for Scenario 5.1 (high beta, steady-state).*

5. Summary and prospects

In this paper, the present state of the modelling work undertaken to prepare the operation and scientific exploitation of JT-60SA has been presented. Some results of the three main areas of this work have been given, i.e., i) examples of NBI and ECRH computations; ii) predictive simulations of JT-60U and JET discharges for transport model comparison; iii) 0.5D

simulations of JT-60SA scenarios. The benchmark of H&CD modules of Japanese and EU integrated modelling codes can be considered as satisfactory. The 0.5D simulations constitute a good basis for preliminary calculations in the MHD and other areas. The validation of predictive modelling for JET and JT-60U is a more challenging task, which should proceed with comparison of the pedestal models, particle transport simulations, as well as fast ions effects, which can play a key role in the establishment of advanced scenarios.

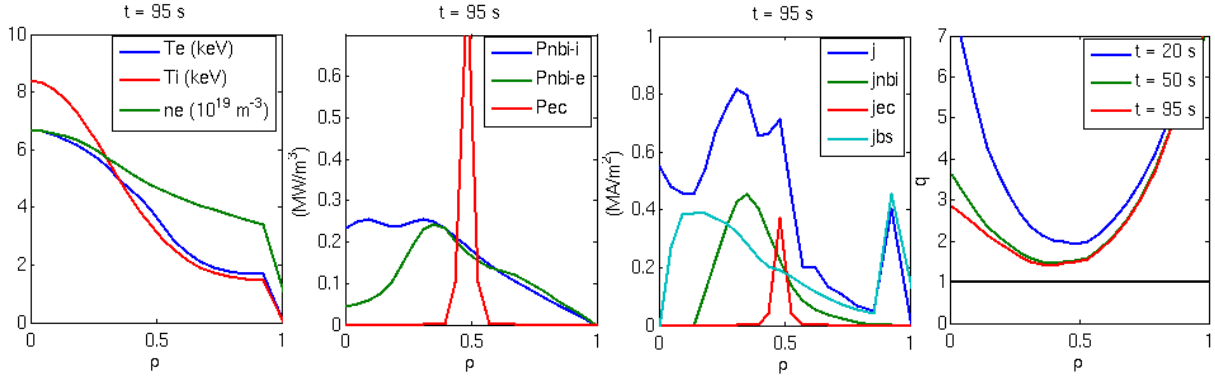

Fig. 9: *As in Fig. 7, for Scenario 5.1 (high beta, steady-state).*

Acknowledgements

This work was supported by EURATOM and carried out within the framework of the European Fusion Development Agreement. The views and opinions expressed herein do not necessarily reflect those of the European Commission.

References

[1] S. Ishida et al., Nucl. Fusion **51**, 094018 (2011)
[2] Y. Kamada et al., Nucl. Fusion **51**, 073011 (2011)
[3] JT-60SA Research Plan -Research Objectives and Strategy Version 3.0 2011, December, *http://www.jt60sa.org/pdfs/JT-60SA_Res_Plan.pdf*
[4] T. Oikawa et al., Proc. 22nd Int. Conf. on Fusion Energy2008 (Geneva, Switzerland, 2008) (Vienna: IAEA) CD-ROM file [IT/P6-5], *http://www-naweb.iaea.org/napc/physics/FEC/FEC2008/html/index.htm*
[5] M. Schneider et al., Nucl. Fusion **51**, 063019 (2011)
[6] J. Johner, Fusion Sci. Techn. **59**, 308 (2011)
[7] J.F. Artaud et al., in 32nd EPS Conf. on Contr. Fusion and Plasma Phys., ECA Vol. **29C**, P1.035 (2005)
[8] J.F. Artaud et al., Nucl. Fusion **50**, 043001 (2010)
[9] K. Tani et al., J. Phys. Soc. Jpn. **50**, 1726 (1981)
[10] M. Schneider et al., Plasma Phys. Control. Fusion **47**, 2087 (2005)
[11] D. Farina, Fus. Sci. Techn. **52**, 154 (2007)
[12] K. Hamamatsu and A. Fukuyama, Fusion Eng. Des. **53**, 53 (2001)
[13] E. Lazzaro, S. Nowak, Plasma Phys. Contr. Fusion **51**, 035005 (2009).
[14] M. Honda and A. Fukuyama, Nucl. Fusion **46**, 580 (2006).
[15] J.E. Kinsey et al.,Phys. Plasmas **12**, 052503 (2005)
[16] Hayashi N. et al., Phys. Plasmas **17**, 056112 (2010).
[17] I. Voitsekhovitch et al., in 39th EPS Plasma Physics Conference, P4.066 (2012)
[18] A. Fukuyama, Plasma Phys. Contr. Fusion **38**, 1319 (1996)
[19] K. Shinya, J. Plasma Fusion Res. **76**, 479 (2000)
[20] D.C. McDonald et al., Nucl. Fusion **47**, 147 (2007)
[21] K. Tani, M. Azumi and R.S. Devoto, J. Comp. Phys. **98**, 332 (1992)
[22] E. Barbato et al., in 39th EPS Plasma Physics Conference, P2.002 (2012)